Proceedings of the 2024
International Symposium on Flexible Automation
ISFA2024
July 21-24, 2024, Seattle, WA

ISFA2024-140948

MACHINE LEARNING-ENHANCED MODEL PREDICTIVE CONTROL FOR INCREMENTAL BENDING OF SKELETAL FIXATION PLATES

Yixue Chen[a], Jianjing Zhang[a], Tyler Babinec[b], Brian Thurston[c], Glenn Daehn[c], David Dean[c], Kenneth Loparo[d], David Hoelzle[b] and Robert X. Gao[a,1]

[a] Department of Mechanical and Aerospace Engineering
Case Western Reserve University
Cleveland, Ohio, USA
[b] Department of Mechanical and Aerospace Engineering
The Ohio State University
Columbus, Ohio, USA
[c] Department of Materials Science and Engineering
The Ohio State University
Columbus, Ohio, USA
[d] Department of Electrical, Computer, and Systems Engineering
Case Western Reserve University
Cleveland, Ohio, USA

ABSTRACT

Skeletal fixation plates are essential components in craniomaxillofacial (CMF) reconstructive surgery to connect skeletal disunions. To ensure that these plates achieve geometric conformity to the CMF skeleton of individual patients, a pre-operative procedure involving manual plate bending is traditionally required. However, manual adjustment of the fixation plate can be time-consuming and is prone to geometric error due to the springback effect and human inspection limitations. This work represents a first step towards autonomous incremental plate bending for CMF reconstructive surgery through machine learning-enabled springback prediction and feedback bending control. Specifically, a Gaussian process is first investigated to complement the physics-based Gardiner equation to improve the accuracy of springback effect estimation, which is then incorporated into nonlinear model predictive controller to determine the optimal sequence of bending inputs to achieve geometric conformity. Evaluation using a simulated environment for bending confirms the effectiveness of the developed approach.

Keywords: Incremental bending, Model predictive control, Gaussian process

1. INTRODUCTION

Craniomaxillofacial (CMF) reconstructive surgery is a critical procedure for patients suffering from conditions that necessitate the removal of bone tissue [1]. This type of surgery is essential for a significant number of patients, aiming not only to restore the basic functions and appearance of the facial structure but also to ensure the patient's quality of life is maintained or enhanced [2].

The complexity of the facial anatomy, including the dimensions of the bone, the function of joints, and the interaction of muscles, underscores the necessity for precise planning and execution of reconstructive procedures [2]. Achieving geometric accuracy in the bending of skeletal fixation plates is therefore paramount to ensure that the reconstructed mandible aligns with the patient's anatomical structure, facilitating optimal recovery and functional outcomes.

Currently, in most cases of significant ~~reconstructive craniomaxillofacial~~ CMF reconstructive surgery, such as cases requiring a bone graft, fixation hardware is prepared by manual bending. As the loads on these plates both during, and in some cases after, the healing of the bones that are held together, the likelihood of post-surgical failure tends to increase, seen in some large studies to be as high as 39% [3]. This approach is not only

[1] Corresponding author: robert.gao@case.edu

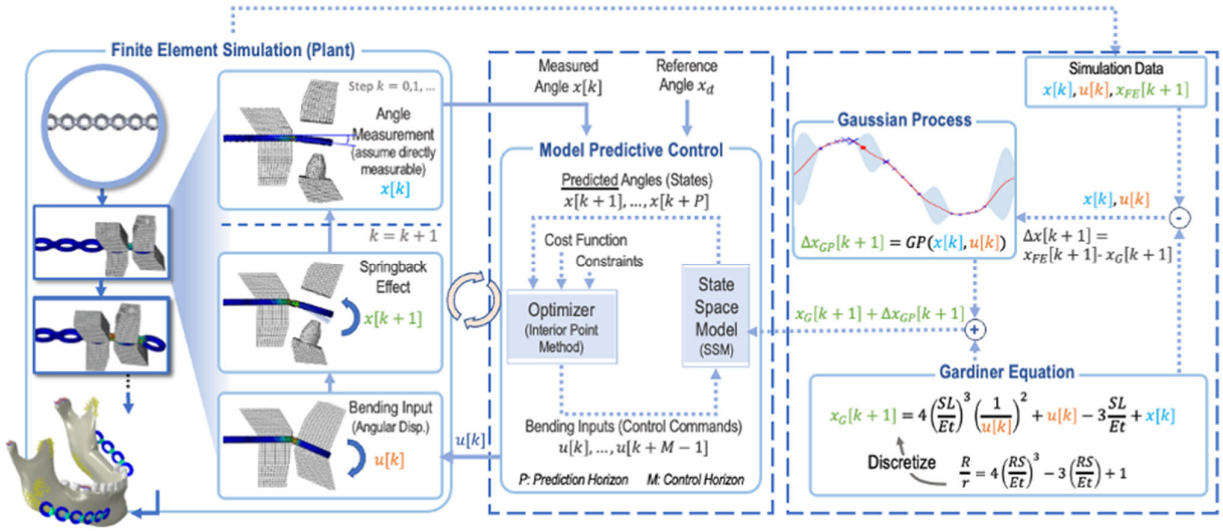

FIGURE 1: Flowchart of skeletal fixation plate bending enabled by machine learning and MPC, with finite element simulation as plant

time-consuming [4] but also subject to inaccuracies, potentially resulting in sub-optimal plate shape and placement [5]. They are primarily due to the inherent limitations of human inspection and the physical properties of the materials involved, notably the springback effect. This refers to the material's tendency to partially return to its original shape after bending due to the hysteresis in the stress strain relationship in plastic deformation, leading to geometric discrepancies between the intended and actual shape of the fixation plate. Such inaccuracies can potentially affect the surgical outcome, making the quest for precision a critical objective in the advancement of CMF reconstructive procedures [6].

Recent advancement of sensing and simulation methods as well as the integration of machine learning into classical model-based control have demonstrated the potential to overcome the limitations in human inspection as well as the difficulties in modeling and predicting material behavior during the manufacturing process, leading to the generation of optimal control input signals to achieve desired manufacturing outcomes. For example, the development of contactless 3D digitization methods based on triangulation, such as structured light, active stereo, and photogrammetry have demonstrated high accuracy in capturing complex geometrics of physical objects [7-8]. More recently, neural rendering, a technique that combines machine learning and physics-based imaging theory has shown the potential to enable low-cost 3D object digitization [9]. The process data generated from these sensors and high-fidelity simulation provides the basis to leverage the power of machine learning for accurate modeling of complex manufacturing processes, such as the effect of laser power and speed on melt pool characteristics in additive manufacturing [10], and the springback effect of sheet metal in incremental sheet forming [11]. The improved accuracy of machine learning-enabled process modeling has led to the improved process control outcomes in manufacturing when combined with control strategies such as model predictive control (MPC) [10-13].

Inspired by these prior works, this study presents an integrated method of machine learning-enabled bending process modeling and nonlinear model predictive control (MPC) to enable the generation of the "optimal" sequence of bending input angles (described as *bending inputs* in the remainder of the paper) to achieve geometric conformity of skeleton fixation plates for CMF reconstructive surgery.

Specifically, Gaussian process (GP) [14] is investigated as the machine learning approach to improve the estimation of the springback effect after the bending load is removed from the plate. The motivation for investigating GP is based on the observation that the nonlinear behavior of springback is observed only in a certain range of bending input, while the effect of the nonlinearity decreases as the bending input increases. GP has shown effectiveness in dealing with such local nonlinear characteristics [15]. In this study, it is implemented as a compensation term for the physics-based Gardiner equation [16], which describes the general springback effect, to capture the nonlinear aspects not encapsulated by the physics-based model.

The GP-enhanced springback model is subsequently incorporated into nonlinear MPC [17-18] to determine the optimal sequence of bending inputs to achieve geometrically accurate plates for CMF reconstructive surgery. The motivation for selecting MPC-based approach is the property of constraint satisfaction [19], which can be critical in avoiding control signals that fall into ranges that are undesirable in practice. The effectiveness of the integrated method is demonstrated in a simulation environment, as shown in Fig. 1. The main contributions of this study include the following:

1) Integration of GP with physics-based Gardiner equation to improve the accuracy of springback prediction in bending of skeletal fixation plates.
2) Incorporation of GP-enhanced prediction into nonlinear MPC to achieve autonomous bending of skeletal fixation plates to support CMF reconstructive procedures.

The rest of the paper is organized as follows: Section 2 presents the theoretical background of Gardiner equation, GP, and nonlinear MPC. In Section 3, the simulation environment for evaluating the developed method is described. The results are presented and discussed in Section 4, and conclusions and future work are summarized in Section 5.

2. THEORETICAL BACKGROUND

Fig. 2 indicates the type of skeletal fixation plate investigated in this study, generally in the form of an elongated plate component of eyelets with webbing in between. These eyelets are for fixing the plate onto the CMF skeleton. As a result, conformity of the plate after incremental bending is crucial to patients' recovery and functional outcomes.

During each bending, one pair of neighboring eyelets are controlled by a pair of robot grippers. Each gripper has a cone-shaped pin that can fully engage with the eyelet geometry when the gripper is closed, ensuring no movement of the eyelet relative to the gripper. The main objective of this study is to determine the optimal sequence of bending inputs to be applied by the grippers such that the corresponding webbing will exhibit accurate deformation conforming to the required local geometry of the patient's CMF skeleton. Achieving this objective requires accurate prediction of the post-springback bending angle (described as *post-springback angle* in the remainder of the paper) that is induced by the hysteresis in the mechanics during plastic deformation and optimization of the sequence of bending inputs to achieve the final geometry.

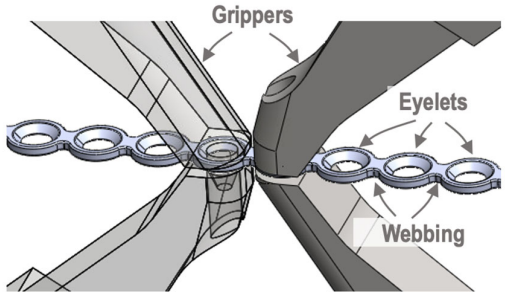

FIGURE 2: Setup for skeletal fixation plate incremental bending. Plate consists of eyelets and webbing and bending is controlled by the rotation torque of a pair of grippers.

2.1 Post-Springback Bending Angle Prediction

In this paper, the springback effect is modeled through the integration of physics-based and data-driven methods. The webbing is first abstracted into a 2D rectangular plate attached to a wall, for which a physics-based Gardiner equation that describes the general springback effect is used [16]. Next, data-driven GP is investigated to compensate for aspects of the springback effect that are not encapsulated in the Gardiner equation [14], such as deviation from the assumptions that are used in its derivation and the geometric complexity in the actual plate (from 2D to 3D), to arrive at a refined, more accurate prediction.

2.1.1 Gardiner Equation

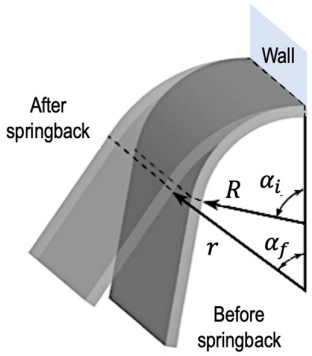

FIGURE 3: Illustration of springback effect in metal bending, adapted from [20]

The Gardiner equation quantifies the relationship between two specific radii of curvature for a 2D plate, one end of which is affixed to a vertical wall (as a slice of the 3D setup shown in Fig. 3). It compares the radius of curvature R when an external load (i.e., bending input) is applied, maintaining the plate at a certain bending angle, to the radius of curvature observed post springback r, after the load is released [16]:

$$\frac{R}{r} = 4\left(\frac{RS}{Et}\right)^3 - 3\left(\frac{RS}{Et}\right) + 1 \tag{1}$$

In Eq. (1), S and E denote the yield stress and the modulus of elasticity of the material, respectively. t is the plate thickness. One of the assumptions of Eq. (1) is that the length of the centerline of the plate L remains constant during the bending process:

$$L = \alpha_i R = \alpha_f r \tag{2}$$

where α_i corresponds to the bending input and α_f is the post-springback angle. Using Eq. (2), Eq. (1) can be expressed as:

$$\alpha_f = 4\left(\frac{SL}{Et}\right)^3 \left(\frac{1}{\alpha_i}\right)^2 + \alpha_i - 3\frac{SL}{Et} \tag{3}$$

which establishes a mathematical relationship between α_f and α_i that is only dependent on the material properties and the dimension of the plate.

Besides the constant centerline assumption, the derivation of Eq. (1) is also based on the elastic-perfectly plastic stress-strain relationship as well as the assumption of proportionality between the strain and the distance from the centerline [16]. While Eq. (1) represents the general springback effect, it is essential that deviations in springback as predicted by this equation from the actual physical bending process that are induced by the violation of the assumptions are properly compensated for to achieve accurate estimation of the springback effect. In this study, machine learning is investigated as a methodology to capture such deviations.

2.1.2 Gaussian Process for Improved Bending Prediction

GP is a machine learning technique where its origin can be traced to Bayesian learning of a single layer neural network with

Gaussian prior imposed on the network weights [14]. Intuitively, GP itself can be considered an infinite dimensional Gaussian distribution over a continuous function, where the function outputs at any finite number of inputs form a multi-dimensional Gaussian distribution.

In this study, the inputs for GP at each bending step k are the *pre-bending angle* $x[k]$ and the applied *bending input* $u[k]$. The output is the deviation between the actual *post-springback angle* $x[k+1]$ and the prediction from the Gardiner equation $x_G[k+1]$. Following [14], the GP-enhanced estimation for springback effect can be written as:

$$x[k+1] - x_G[k+1] \sim GP(0, K([x[k], u[k]], [x'[k], u'[k]])) \quad (4)$$

In Eq. (4), K is the covariance matrix that quantifies the correlation of the deviation in post-springback angle for two different inputs $x[k], u[k]$ and $x'[k], u'[k]$ in the GP-predictor.

Denoting the training inputs consisting of pairs of $x[k], u[k]$ as X_{train}, and the training outputs (from FEM) consisting of the deviations between pairs of $x[k+1]$ and $x_G[k+1]$ as $\boldsymbol{y}_{\text{train}}$, similarly for testing inputs X_{test} and outputs $\boldsymbol{y}_{\text{test}}$, the prediction of GP for $\boldsymbol{y}_{\text{test}}$ can be computed as the posterior distribution of $\boldsymbol{y}_{\text{test}}$ given $\boldsymbol{y}_{\text{train}}$ [14]:

$$p(\boldsymbol{y}_{\text{test}} | \boldsymbol{y}_{\text{train}}) \sim N(BC^{-1}\boldsymbol{y}_{\text{train}}, A - BC^{-1}B^T) \quad (5)$$

where A is the covariance matrix computed using samples from X_{test}, C is the covariance matrix computed using samples from X_{train}, and B contains the correlations among samples between X_{test} and X_{train}. In this study, the radial basis function (RBF) covariance function is used to compute the correlation between two distinct inputs, analogous to the RBF kernel that is widely used in the machine learning to resolve nonlinearity:

$$k(X, X') = \sigma^2 \exp\left(-\frac{1}{2l^2}\|X - X'\|^2\right) \quad (6)$$

In Eq. (6), σ and l are the two GP parameters that will be optimized using the maximum likelihood estimation technique [14]. Intuitively, $BC^{-1}\boldsymbol{y}_{\text{train}}$ in Eq. (5) can be considered as a data-driven compensation term to refine the predictions that are derived from the Gardiner equation.

For a pair of new inputs $x[k], u[k]$, the predicted post-springback angle will be the mean of the posterior distribution computed using Eq. (5) plus the prediction from the Gardiner equation $x_G[k+1]$, which is itself a function of $x[k]$ and $u[k]$.

2.2 Nonlinear MPC for Incremental Bending

With the GP-enhanced predictive model for post-springback angle, nonlinear MPC is investigated to generate an optimal sequence of bending inputs to incrementally achieve the desired geometry for each pair of eyelets. Specifically, nonlinear MPC is formulated as [21]:

$$\min_U \sum_{j=0}^{P-1} Q\left(x[k+j] - x_{ref}\right)^2 + R(u[k+j])^2 + Q_f\left(x[k+P] - x_{ref}\right)^2 \quad (7a)$$

$$\text{s.t: } x[k+1] = F(x[k], u[k]) \quad (7b)$$

$$u_{min} \le u[k] \le u_{max} \quad (7c)$$

$$x_{min} \le x[k] \le x_{max} \quad (7d)$$

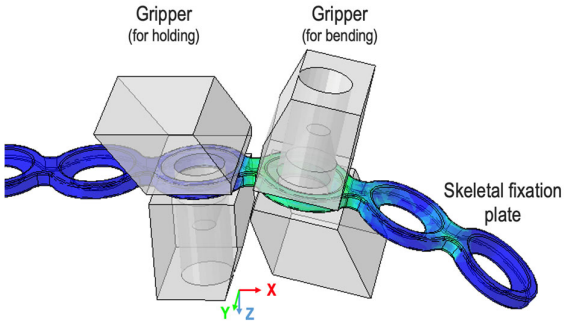

FIGURE 4: FE simulation of bending skeletal fixation plate

where k indexes the bend angle and bend input pairs to be evaluated, $U = \{u[k], \dots, u[k+P-1]\}$ denotes the sequence of bending inputs over the prediction horizon P. The GP-enhanced predictive model Eq. (4) is converted into the model given in Eq. (7b) by moving $x_G[k+1]$ to the right-hand side. The terms x_{min}, x_{max}, u_{min} and u_{max} represent the lower and upper bounds for the variables x and control inputs u, respectively. The cost function to be minimized during the optimization process consists of three terms as shown in Eq. (7a), with the first two representing the running cost and the last term is the terminal cost, respectively. The parameters Q, R, and Q_f are the penalizing weights for the corresponding terms.

The optimal bending input $u[k]$ at each iteration k is determined by solving the nonlinear MPC problem through an Interior Point OPTimizer (IPOPT) solver using CasADi, which is an open-source numerical optimization library written in Python [22]. The first step of the optimized control sequence U is applied as bending input to the incremental bending process, and then the optimization problem is solved again from the new pending angle that results.

3. EXPERIMENTAL EVALUATION

The developed approach is evaluated in a finite element (FE)-based simulation environment. The geometries of the gripper and the skeletal fixation plate are first imported, and training data is generated in the form of triplets $(x[k], u[k], x[k+1])$ by varying $x[k], u[k]$ and recording the simulated $x[k+1]$. The training data is used to train the GP model before it is implemented with nonlinear MPC to determine the optimal bending inputs.

3.1 Finite Element Simulation

FE simulation of incremental bending is implemented in Abaqus as shown in Fig. 4, using a slightly simplified gripper geometry based on what is shown in Fig. 2. At each bending step, a pair of neighboring eyelets are clamped by a pair of grippers, where one of the grippers plays the role of "holding" the eyelet during bending, and the other gripper rotates around the y-axis

to apply the bending input based on the results from nonlinear MPC. After each bending action, the gripper for bending is released, allowing the actual post-springback angle to be measured, which serves as the pre-bending angle in the next step. Once the geometry of the current pair of eyelets is deemed satisfactory, the grippers shift to the next pair of eyelets and whole bending control process repeats.

In FE simulation, the pair of grippers are treated as rigid bodies and hexahedral meshes are used to reduce the computational cost [23]. The deformable skeletal fixation plate is generated with tetrahedral meshes using seed 0.19, as shown in Fig. 5 and Table 1.

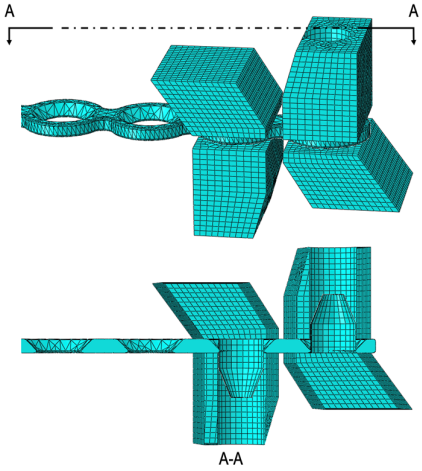

FIGURE 5: Geometry and mesh of gripper and plate

Table 1 FE simulation parameters

	Element type	Deformable status
Fixation plate	Tetrahedral	Deformable
Grippers	Hexahedral	Rigid

When the gripper for holding engages with and clamps the corresponding eyelet, it constrains all active structural degrees of freedom within the region of the clamped eyelet. Encastre boundary condition is thus applied to that specific region [24]. A specific angular displacement is applied to the center point of the cross-section at the end of the deformation region to simulate the process of the gripper applying the bending input to the plate. Fig. 6 shows the boundary condition in FE simulation and the point of interest used to collect data.

In this study, aluminum alloy 6061 is evaluated as the material for bending, and its material properties are shown in Table 2. A total of 238 data samples (i.e., triplets) have been collected from simulation using the FE program. For data collection, specific considerations were given on the region where elastic-plastic transition occurs, and on the differences between calculations from the Gardiner equation and simulation from the FE model. An 80-20 allocation was chosen for the training and validation data sets for GP model's training and validation. Four trials in total were carried out.

Table 2 Material properties of Al 6061

Density	Young's modulus	Poisson ratio	Yield stress
2.7g/cm^3	68.9 GPa	0.33	276 MPa

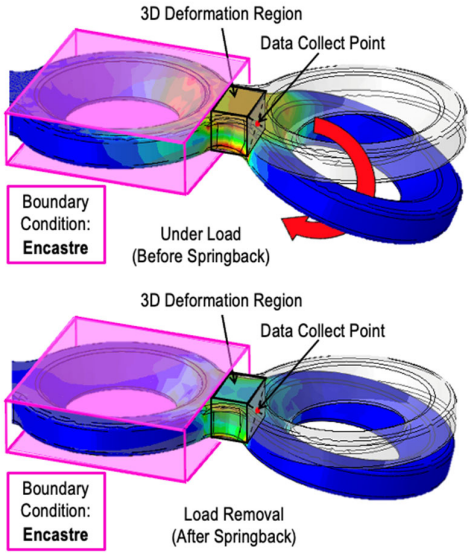

FIGURE 6: Boundary condition and point for data collection

4. RESULTS AND DISCUSSION

4.1 GP-Enhanced Model Performance

The data samples are first displayed along with prediction from the Gardiner equation in Fig. 7. To facilitate visualization, the triplet $(x[k], u[k], x[k+1])$ is converted into a 2D plot by using the delta between the post-springback angle $x[k+1]$ and the pre-bending angle $x[k]$ as points on the y-axis while the bending input $u[k]$ as points on the x-axis.

It is noted from Fig. 7 that an elevated level of nonlinearity is observed in the bending input range between -10 degrees and 10 degrees where the Gardiner equation prediction shows a substantial deviation from FE data. This is because plastic deformation behaves unsteadily during the entire bending process [25]. Additionally, the nonlinearity decreases as the amplitude of the bending input increases, leading to improved matching between the FE data and the prediction from the Gardiner equation.

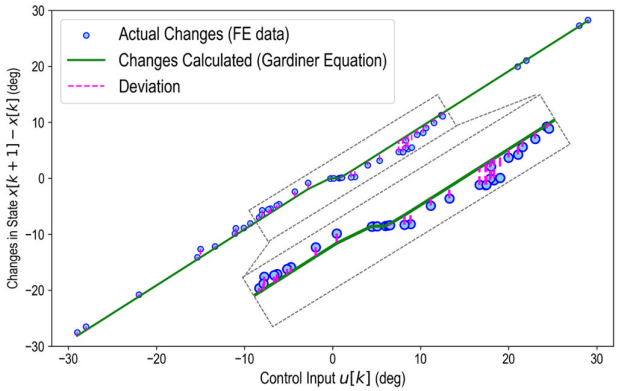

FIGURE 7: Comparison of FE data and Gardiner results

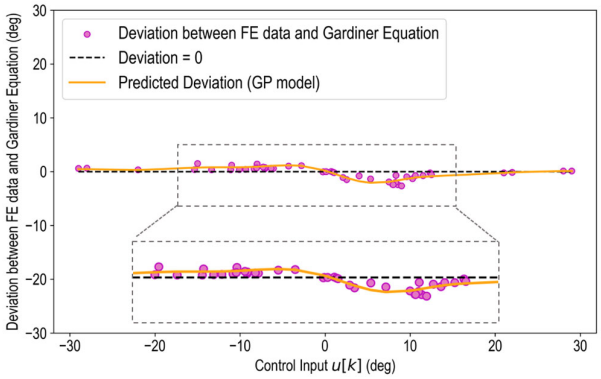

FIGURE 8: GP predicted deviation between FE & Gardiner equation

Fig. 8 plots both the deviation between the FE data and the predictions from Gardiner model (as shown by the magenta dashed line in Fig. 7) and the GP prediction of this deviation. It is noted that GP predictions are closely aligned with the FE data points, indicating its good performance in compensating for the Gardiner model. Numerical results from 4-fold GP training and validation indicate that the mean of the root mean squared error (RMSE) for predicting post-springback angle using GP-enhanced model is 0.007 rad (approximately 0.4 deg). This represents a 63.6% improvement over the result from using the Gardiner model alone, which shows an RMSE of 0.020 rad (approximately 1.1 deg). This confirms the effectiveness of GP as a machine learning method to enhance predictive modeling of nonlinear behavior in the plate bending process.

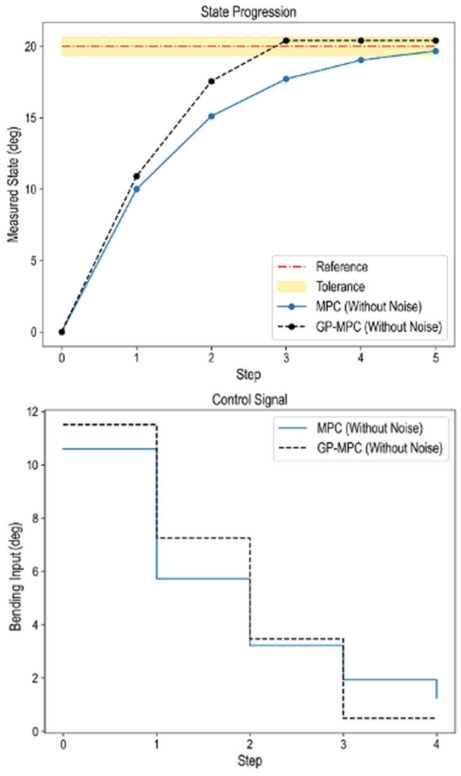

FIGURE 9: GP-MPC vs. MPC (without noise)

4.2 MPC Performance

The MPC methodology is evaluated in terms of its ability to achieve a target bending angle of 20 degrees for one individual pair of eyelets. With the GP-enhanced model, MPC iteratively updates the bending input based on the feedback of the measured post-springback angle at each step. The parameters for GP-MPC are shown in Table 3.

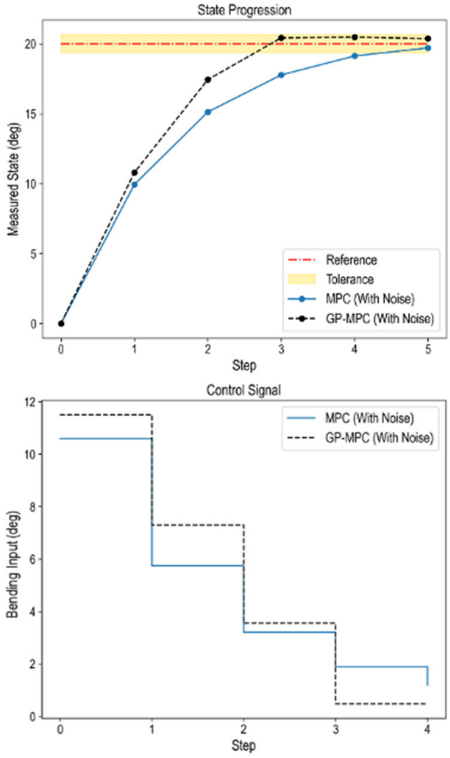

FIGURE 10: GP-MPC vs. MPC (with noise)

Table 3 Parameters of GP-MPC

Q	R	Q_f	u_{min}/u_{max}(deg)	x_{min}/x_{max}(deg)	Tolerance (deg)
10	1	10	$0/+30$	$0/+20$	± 0.65

Fig. 9 shows the result comparison between MPC using only the Gardiner equation alone as the model (denoted as MPC) and the MPC using the GP-enhanced model (denoted as GP-MPC). In the configuration of the two MPC systems, the prediction horizons were set to 2 steps, and the control horizons are set at 1 step. The maximum number of steps for MPC to reach the reference angle was set to 5 for the simulation. It is noted that the GP-MPC benefits from the more accurate prediction obtained using GP-enhanced model as reflected in its convergence to the target bending angle at a faster rate than the MPC with Gardiner equation alone (3 steps by GP-MPC as compared to 5 by MPC, an improvement of 40%). The same comparison is carried out under measurement noise with zero mean and a standard deviation of 0.08 deg, based on the understanding that the measurement noise is Gaussian distributed and the sensor's measurement accuracy is given by the manufacturer as 0.08 deg).

As shown in Fig. 10, similar behavior in convergence of the two controllers is observed. This confirms the effectiveness of the machine learning-enhanced model in improving the MPC's performance. The steady-state error of the GP-MPC is about 0.006 rad (approximately 0.3 deg), either with or without noise. Furthermore, the consistency of the MPC's performance under noise was evaluated, for which ten test runs were conducted. The low error bars as shown in Fig. 11 indicate stable performance of the controller.

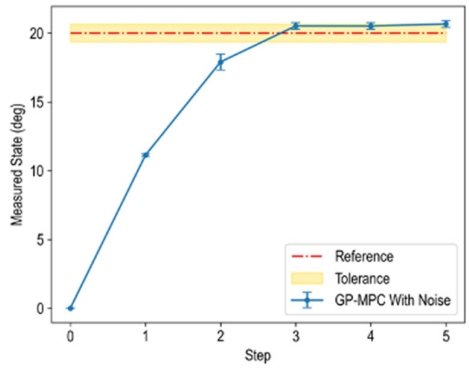

FIGURE 11: Results of 10 runs of GP-MPC with noise

Finally, the effect of increased level of the control effort on the its performance is evaluated by increasing the ratio of the parameter Q/R (the symbol "Q" denotes the combined effect of both Q and Q_f) in the cost function, from 10 to 1,000. The increase makes the cost function biased towards penalizing the discrepancy between the measured post-springback angle and the target bending angle, instead of the amplitude of the control bending inputs. Figures 12 and 13 illustrate that the GP-MPC, when employing a more aggressive control strategy, achieves convergence to the target angle more rapidly with and without noise. Both the GP-MPC with an aggressive control strategy and the one with a non-aggressive control strategy demonstrate the capability of accommodating uncertainties such as noise and ensuring reliable operation even under suboptimal conditions. However, the speed benefit when compared to MPC is limited with the 100-times reduction in R.

5. CONCLUSIONS AND FUTURE WORK

In an effort to ensure the optimal fit and function of CMF reconstructive surgery by achieving geometric conformity of the skeleton fixation plate, an integrated method of machine learning-enhanced springback predictive modeling and nonlinear MPC is presented. Specifically, a Gaussian process (GP) model is investigated to compensate for limitations in the physics-based Gardiner equation to arrive at a more accurate prediction of the post-springback angle in plate bending. The GP-enhanced prediction then serves as the model in the nonlinear MPC formulation that is used to generate an optimal sequence of bending inputs to achieve the desired geometry of the skeleton fixation plate.

In the simulated case study, it is shown that the GP-enhanced model outperforms the Gardiner equation in predicting post-springback angle, reducing the prediction error from 1.1 degrees to 0.4 degrees, a 63.6% reduction. Additionally, nonlinear MPC with GP-enhanced model also demonstrated faster convergence to the desired geometry as compared to the nonlinear MPC with

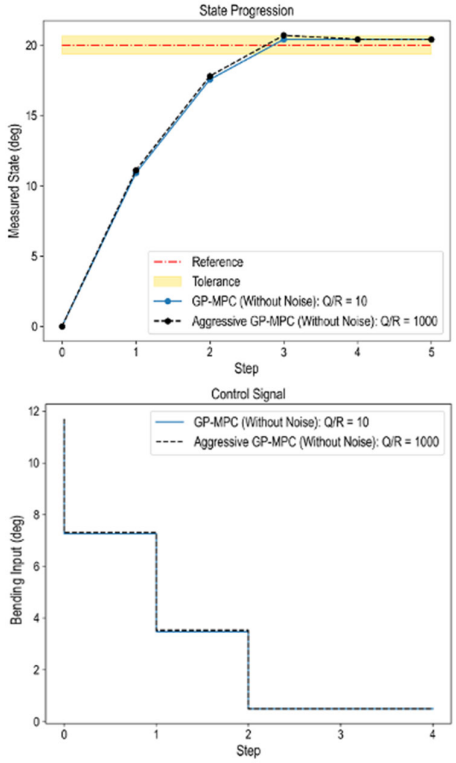

FIGURE 12: GP-MPC with increased ratio of cost function parameter Q/R (without noise)

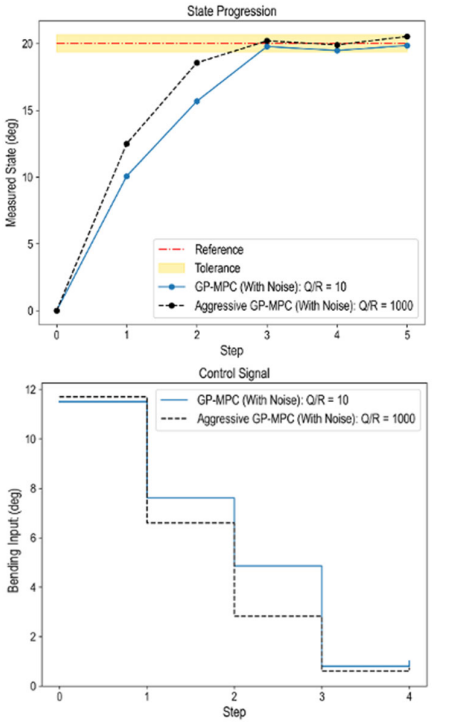

FIGURE 13: GP-MPC with increased ratio of cost function parameter Q/R (with noise)

Gardiner equation alone, reducing the needed steps from 27 to 16, representing a 40.7% reduction.

While the GP-MPC has demonstrated the ability to achieve the desired bending angle in fewer steps than the nonlinear MPC, repeated bending may lead to work hardening and, consequently, fatigue failure after surgery [5]. Therefore, minimizing the number of steps required to achieve the desired angle will be a focus in the ongoing development of MPC design. Future work will also investigate optimized GP models, such as sparse GP [26] to further improve the computational efficiency of GP in training and testing and reduce the duration needed to realize incremental bending. Additionally, stochastic MPC formulation will be considered based on the characteristic of GP-enhanced model. Future work will also provide in-depth investigation of the effect of nonlinear MPC's parameters on the controller's performance, as well as on demonstrating the developed method using a physical robot to advance the state of point-of-care manufacturing (PCOM).

ACKNOWLEDGEMENTS

The authors gratefully acknowledge support from the NSF Engineering Research Center for Hybrid Autonomous Manufacturing: Moving from Evolution to Revolution (ERC-HAMMER) under award EEC-2133630.

REFERENCES

[1] Shayesteh Moghaddam, N., Taheri Andani, M., Amerinatanzi, A., Haberland, C., Huff, S., Miller, M., Elahinia, M. and Dean, D., 2016. Metals for bone implants: Safety, design, and efficacy. Biomanufacturing Reviews, 1, pp.1-16.

[2] Zeller, A.N., Neuhaus, M.T., Weissbach, L.V.M., Rana, M., Dhawan, A., Eckstein, F.M., Gellrich, N.C. and Zimmerer, R.M., 2020. Patient-specific mandibular reconstruction plates increase accuracy and long-term stability in immediate alloplastic reconstruction of segmental mandibular defects. Journal of Maxillofacial and Oral Surgery, 19, pp.609-615.

[3] Van Der Rijt, E.E.M., Noorlag, R., Koole, R., Abbink, J.H. and Rosenberg, A.J.W.P., 2015. Predictive factors for premature loss of Martin 2.7 mandibular reconstruction plates. British Journal of Oral and Maxillofacial Surgery, 53(2), pp.121-125.

[4] Mazzoni, S., Marchetti, C., Sgarzani, R., Cipriani, R., Scotti, R. and Ciocca, L., 2013. Prosthetically guided maxillofacial surgery: evaluation of the accuracy of a surgical guide and custom-made bone plate in oncology patients after mandibular reconstruction. Plastic and reconstructive surgery, 131(6), pp.1376-1385.

[5] Vazquez-Armendariz, J., Olivas-Alanis, L.H., Mahan, T., Rodriguez, C.A., Groeber, M., Niezgoda, S., Morris, J.M., Emam, H., Skoracki, R., Cao, J. and Ripley, B., 2023. Workflow for Robotic Point-of-Care Manufacturing of Personalized Maxillofacial Graft Fixation Hardware. Integrating Materials and Manufacturing Innovation, pp.1-13.

[6] Weitz, J., Bauer, F.J.M., Hapfelmeier, A., Rohleder, N.H., Wolff, K.D. and Kesting, M.R., 2016. Accuracy of mandibular reconstruction by three-dimensional guided vascularised fibular free flap after segmental mandibulectomy. British Journal of Oral and Maxillofacial Surgery, 54(5), pp.506-510.

[7] Jacobs, L., Dvorak, J., Cornelius, A., Zameroski, R., No, T. and Schmitz, T., 2023. Structured light scanning artifact-based performance study. Manufacturing Letters, 35, pp.873-882.

[8] Galantucci, L.M., Pesce, M. and Lavecchia, F., 2015. A stereo photogrammetry scanning methodology, for precise and accurate 3D digitization of small parts with sub-millimeter sized features. CIRP Annals, 64(1), pp.507-510.

[9] Zhang, J., Liu, S., Gao, R. and Wang, L., 2023. Neural rendering-enabled 3D modeling for rapid digitization of in-service products. CIRP Annals.

[10] Asadi, F., Olleak, A., Yi, J. and Guo, Y., 2021. Gaussian process (gp)-based learning control of selective laser melting process. In 2021 American Control Conference (ACC) (pp. 508-513).

[11] Lu, H., Kearney, M., Li, Y., Liu, S., Daniel, W.J. and Meehan, P.A., 2016. Model predictive control of incremental sheet forming for geometric accuracy improvement. The International Journal of Advanced Manufacturing Technology, 82, pp.1781-1794.

[12] Ay, M., Schwenzer, M., Stemmler, S., Rüppel, A., Abel, D. and Bergs, T., 2022, July. Practical Nonlinear Model Predictive Control of a CNC Machining Center with Support Vector Machines. In 2022 IEEE/ASME International Conference on Advanced Intelligent Mechatronics (AIM) (pp. 1625-1631). IEEE.

[13] Allwood, J.M., Duncan, S.R., Cao, J., Groche, P., Hirt, G., Kinsey, B., Kuboki, T., Liewald, M., Sterzing, A. and Tekkaya, A.E., 2016. Closed-loop control of product properties in metal forming. CIRP Annals, 65(2), pp.573-596.

[14] Williams, C.K. and Rasmussen, C.E., 2006. Gaussian processes for machine learning (Vol. 2, No. 3, p. 4). Cambridge, MA: MIT press.

[15] Zhang, J., Liu, C. and Gao, R., 2022. Physics-guided Gaussian process for HVAC system performance prognosis. Mechanical Systems and Signal Processing, 179, p.109336.

[16] Gardiner, F.J., 1957. The spring back of metals. Transactions of the American Society of Mechanical Engineers, 79(1), pp.1-7.

[17] Gros, S., Zanon, M., Quirynen, R., Bemporad, A. and Diehl, M., 2020. From linear to nonlinear MPC: bridging the gap via the real-time iteration. International Journal of Control, 93(1), pp.62-80.

[18] Kamel, M., Burri, M. and Siegwart, R., 2017. Linear vs nonlinear mpc for trajectory tracking applied to rotary wing micro aerial vehicles. IFAC-PapersOnLine, 50(1), pp.3463-3469.

[19] Hewing, L., Wabersich, K.P., Menner, M. and Zeilinger, M.N., 2020. Learning-based model predictive control: Toward safe learning in control. Annual Review of Control, Robotics, and Autonomous Systems, 3, pp.269-296.

[20] CUSTOMPART.NET: Spring Back Calculator. Available online: https://www.custompartnet.com/calculator/bending-springback (accessed on 02-09-2024).

[21] Zanelli, A., Quirynen, R., Jerez, J. and Diehl, M., 2017. A homotopy-based nonlinear interior-point method for NMPC. IFAC-PapersOnLine, 50(1), pp.13188-13193.

[22] Nonlinear programming, https://web.casadi.org/docs/ (accessed on 02-10-2024)

[23] Karpik, A., Cosco, F. and Mundo, D., 2023. Higher-Order Hexahedral Finite Elements for Structural Dynamics: A Comparative Review. Machines, 11(3), p.326.

[24] Smith, M 2009, ABAQUS/Standard User's Manual, Version 6.9. Dassault Systèmes Simulia Corp, Providence, RI.

[25] Li, H., Yang, H., Song, F.F. and Li, G.J., 2013. Springback nonlinearity of high-strength titanium alloy tube upon mandrel bending. International Journal of Precision Engineering and Manufacturing, 14, pp.429-438.

[26] Luo, H., Nattino, G. and Pratola, M.T., 2022. Sparse additive Gaussian process regression. Journal of Machine Learning Research, 23(61), pp.1-34.